Fabrication, characterization and application of flat sheet PAN/CNC nanocomposite nanofiber pressure-retarded osmosis (PRO) membrane

Mehmet Emin Paşaoğlu[a,b], İsmail Koyuncu[a,b],*

[a]*Istanbul Technical University Civil Engineering Faculty, Environmental Engineering Department, 34469 Maslak/Sarıyer/Istanbul, Turkey, emails: koyuncu@itu.edu.tr (İ. Koyuncu), mpasaoglu@itu.edu.tr (M. Emin Paşaoğlu)*
[b]*National Research Center on Membrane Technologies (MEM-TEK), Advanced Technology Center, 34469 Maslak/Sarıyer/Istanbul, Turkey*

ABSTRACT

The aim of this work is to fabricate nanocellulose based nanofiber pressure-retarded osmosis (PRO) via electrospinning technique. PRO process requires high performance, high flux, high rejection and resistant membranes. Conventional phase-inversion membranes are not enough to perform the required water fluxes. Because of this reason, alternative membrane fabrication methods need to be found. Nowadays, electrospinning is the best alternative method to fabricate strong enough nanofiber PRO membranes resistant process operation pressure while providing high flux and high rejection rates. In this study, cellulose nanocrystals (CNC) added polyacrylonitrile (PAN) nanofiber pressure retarded membranes successfully fabricated via tailor-made flat sheet fabrication equipment. According to the scanning electron microscopy, Fourier-transform infrared spectroscopy and dynamic mechanical analysis, parameter and contact angle analysis results, it is concluded that PAN and CNC provided a complete mixture and the addition of CNC increased the mechanical strength in the PAN membranes which is the crucial phenomena in PRO applications. The newly developed membrane can achieve a higher PRO water flux of 300 LMH, using a 1 M NaCl draw solution and deionized water feed solution. The corresponding salt flux is only 1.5 gMH. The reverse flux selectivity represented by the ratio of water flux to reverse salt flux (J_w/J_s) was able to be kept as high as 200 L/g for PRO operation. To the best of our knowledge, the performance of the current work developed membrane is superior to all PRO membranes previously reported in the literature.

Keywords: Electrospinning; Pressure retarded osmosis; Nanocellulose; Flat-sheet nanofiber membrane fabrication; Filtration

1. Introduction

Due to the continuous increase in the cost of fossil fuels power generation has drawn lots of attention. Power generation from renewable resources forcing many countries to reduced fossil fuel consumption. Companies that have low environmental performance face strict regulations and high penalties. Because of limited energy efficiency and solar and wind energy their performance is affected by the wind and solar radiation. In order to find robust technologies continuous research is necessary [1].

Worldwide energy demand is mainly based on fossil fuel-based technology. Researchers try to find alternative energy sources such as solar, wind, biomass, hydropower, tidal power, ocean thermal energy conversion, etc. because of fossil fuel's environmental and political impacts. Many of these technologies promising technologies have geographic limitations or natural intermittence. In addition to alternative sources recently salinity gradient power has the advantage. It is possible to exist naturally occurring salinity gradients all over the world where freshwater meets saline water. Salinity gradients can be harnessed using osmosis.

For example, ocean water and river water have about 270 m of hydraulic head chemical potential difference [2]. The global potential for power generation is estimated at 1.4–2.6 TW from which approximately 980 GW can be effectively harnessed with an appropriate system design [2,3]. Numerous methods have been developed to generate electricity by harnessing salinity gradients such as batteries, supercapacitor flow cells [4], reverse electrodialysis [3,5] osmotic microbial fuel cells and other hybrid technologies [3]. Among all mentioned methods pressure-retarded osmosis (PRO) is one of the most promising [3–8].

The electrospinning process can be described as a process in which a high electrostatic field (mainly DC voltage) is applied to form nanofibers with a variety of properties. Applying pressure by means of a syringe pump to a polymeric solution or melt, a pendant drop of a polymeric solution at the tip of the capillary tube (spinneret) forms. The tip of the capillary is integrated into an electrode and the other side of the electrode is integrated with a high DC voltage. Electrical forces draw this pendant drop into a hemispherical shape known as a Taylor cone. The viscosity of the polymeric solution is one of the most important parameters forming a stable jet originates from the Taylor cone. When the equilibrium between electrostatic forces and surface tension exists, a Taylor cone is formed. As soon as the required electrostatic field applied and surpasses surface tension, an extended Taylor cone is formed and a jet is originated. Polymer jet which is originated from the Taylor cone travels linearly for some distance, generally 1–2 cm also known as the jet length. Polymer jet forms a whipping or spiral motion termed as the bending instability. Bending instability causes plastic deformation which makes fibers very long and thin. Most of the solvent evaporates and finally collected on a grounded collector screen during the jet's flight from the capillary tube [9].

Cellulose, one of the most important natural polymers, is an unceasing raw material and the main source of sustainable materials on the industrial scale. The global quantity of cellulose reaches 700.000 billion tons, but only 0.1 billion tons of cellulose is currently being used for the production of paper, textiles, pharmaceutical compounds and others. Cellulose, hemicellulose and lignins are larger units known as elementary fibrils or microfibrils brought together by biomass with about 36 individual cellulose molecules. Elementary fibrils or microfibrils are packed into larger units called micro-fibrillated cellulose.

The production of cellulosic fibers in nano-dimensions has promising properties such as high mechanical performance, hydrophilicity, broad chemical modification, the formation of versatile semi-crystalline fiber morphologies, large surface area and low-density properties, besides renewability and biodegradability. The cellulosic source and the processing conditions dimensions, preparation methods and functions are changeable. Thus, generally, it is possible to categorize nanocellulose into three main groups [10].

The production of PRO membranes has progressed more gradually as opposed to forward osmosis (FO) membranes because of the high pressure added to the draw solution. Many FO membranes can collapse during PRO operations or become severely deformed. The PRO flat-sheet membrane modules need spacers to preserve flow channels and facilitate the mass transfer. As well as causing hydraulic pressure losses along the flow channels, the feed spacers eventually deform PRO membranes under high-pressure operations.

In order to increase membrane robustness, polymeric membranes are not enough to sustain that much pressure. It is possible to increase Young's Modules of nanofiber membranes [11]. Cellulose has been known for about 150 years and is a renewable and biodegradable polymer and has for a long time been used as an energy source, building material, and clothing. By chemical modification on the cellulose polymers, cellulose derivatives such as cellulose ethers and cellulose ester can be prepared, which have opened up for many novel material and applications for cellulose such as coatings, films, membranes, new building materials, drilling techniques, pharmaceuticals, and food products. Also, the regeneration process of cellulose has contributed to novel techniques such as the spinning of fibers and the viscose process.

The natural fiber strength and stiffness in cellulose fibers come from the formation of the microfibrils. Microfibrils have a wide range from 2 to 30 nm depending on the cellulose source and a length that can be several micrometers. The fibrils are assembled into long threadlike bundles of cellulose molecules stabilized by hydrogen bonds [12–14].

In this study, researchers were done on strengthening and also performance-enhancing effects (flux increase as a result of higher hydrophilicity) of the cellulose nanocrystals (CNC) addition on the nanofiber thin-film composite (TFC)-PRO membrane produced from polyacrylonitrile (PAN) polymer were investigated. Firstly, pure PAN-based and PAN/CNC doped nanofiber membranes were fabricated. Then, TFC coating was made on the produced membranes and turned into a PRO membrane. In order to find the optimum CNC addition to the PAN polymer matrix while forming the most durable PRO membrane, different CNC ratios were prepared. Before the fabricated membranes were used, their characterizations were made and performances are compared. Besides, CNC also makes the composite structure more hydrophilic, allowing an increase in net flux.

2. Material and methods

PAN polymer was used to fabricate nanofiber composite membrane from Sigma-Aldrich (USA) as nanofiber base material and nanocellulose addition arranged as 1%, 2%, 5% and 10% wt./wt. N,N-Dimethylformamide (DMF) was used as a solvent from AK-KİM Chemicals (Turkey). A tailor-made flat sheet electrospinning device was used for the fabrication of nanofiber membranes over polyester nonwoven support and crystal nanocellulose brought from BGB Company (Canada).

2.1. Fabrication of nanocellulose added support membranes

Dried at 70°C overnight in a vacuum oven, PAN (12 wt.%) with a definite dissolved in N,N-dimethylacetamide by stirring at 30°C for about 48 h. The electrospinning setup (Fig. 1) was used to fabricate nanofiber substrate onto a polyester (PET) non-woven support. The electrospinning conditions were as follows: spinning solution flow rate of 4 mL/min; voltage 30 kV; tip-collector distance, 19 cm; and
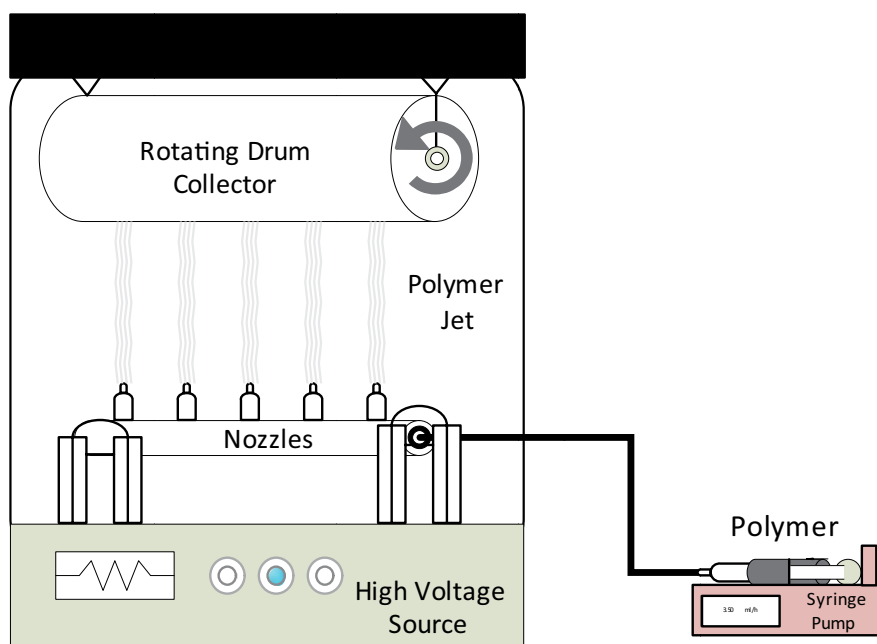
Fig. 1. Schematic of electrospinning setup used for nanofiber membrane fabrication.

temperature, 25°C. High voltage is applied to nozzles and polymer solution pressurized by a syringe pump.

Five different membranes are made including CNC addition starting from 0%, 1%, 2%, 5% and 10% respectively to PAN polymer.

2.2. Fabrication of thin-film composite membranes

The membrane substrate was held in distilled water 24 h for improved wetting before synthesizing the TFC coating. Removal of air bubbles used for processing the *m*-phenylenediamine (MPD) solution, 10 min with nitrogen gas carried out to remove all the remaining compounds. Once the 1,3,5-benzenetricarbonyl trichloride (TMC) solution bottles were washed, a small amount of hexane was used to wash and extract any residual distilled water and additional TMC applied to hexane during mixing for even distribution and homogeneity.

The formation of an interfacial multi-polymerization layer on top of electrospun substrates between the MPD and TMC is shown in Fig. 2.

The TFC membrane coating procedure is given in Table 1.

Fabricated membranes are stored in distilled water after post-treatment. A schematic view of the fabrication steps is shown in Fig. 3.

2.3. Scanning electron microscopy (SEM) examination

Advances were made possible in membrane structure analysis by microscopic techniques such as scanning electron microscopy (SEM) [15]. SEM is now almost a standard tool for the investigation of surface properties of membranes, including surface topography, alteration of the surface by modification, biomacromolecule adsorption, fouling, etc. [16].

2.4. Pressure retarded osmosis setup

For the experiment, water flow and reverse leakage of salt have been measured. Fig. 4 demonstrates the size of the TFC membranes produced from the electrospun-PAN/CNC based PRO system. The membrane cell is divided into rectangular channels with a significant membrane surface area of 0.0058 m² on both sides of the membrane (length 9 cm, width 6.45 cm and depth 0.3 cm). In order to prevent inconsistencies between the feed solution and draw solution sources, 2 O-rings were placed on the outer perimeter of the cell. A medium spacer made of 45 mil (1.14 mm) diamond-type polypropylene screen. The salt concentration changes in both the feed and draw solutions measured by electrical conductivity meter. Feed side weight changes were recorded with digital balance. As a consequence of water extract from the feed solution side, the initial concentration of the drawing solution decreases. PRO tests were performed using 1 M NaCl as draw solution and deionized (DI) water as the feed solution under standard room temperature. A schematic draw of the PRO test setup is shown in Fig. 4.

3. Results and discussion

3.1. SEM images of the fabricated membranes

The morphological structure of the fabricated nanofiber substrates and TFC-PRO membranes was examined with SEM analysis in Figs. 5 and 6, respectively (Quanta FEG 250, Czech Republic).

The configuration and the inherent properties of the support layer directly affect the structure and efficiency of the TFC membranes. In general, the "ridge-and-valley" (also referred to as "leaf-like") morphology of the TFC membrane shown in Fig. 6 is a well-known feature of interfacial polymerized polyamide (PA) membranes. As already mentioned,
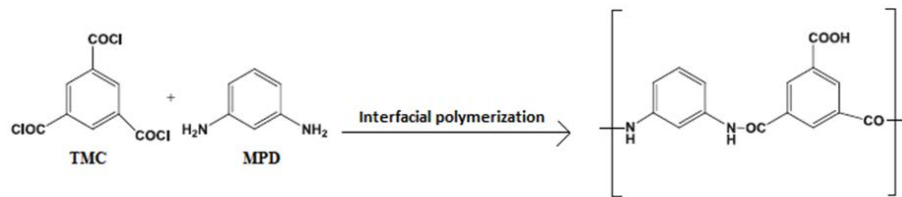
Fig. 2. Interfacial polymerization reaction scheme to form the polyamide separation layer [16].

Table 1
Thin-film composite membrane coating procedure

TMC concentration, %	0.15
TMC duration, min	4
MPD concentration, %	3.5
MPD duration, min	15
Air dry, min	1
Oven dry at 70°C, min	5

the benefit of microscopic use is that the membrane structure is clearly notified [18]. In order to see TFC-PRO membrane structure, SEM images are provided in Fig. 7. The addition of CNC into PAN polymer, it is found that the enhanced hydrophilic nature of polysulfone substrate upon the addition of hydrophilic could form a "nodular" film while the increasing amount of CNC into the PAN matrix could result in the formation of some spherical and cylindrical shapes on PA layer. In general, the most effective TFC-PRO membranes provide fairly hydrophobic support for generating a thin PA film with strong salt rejection. However, in the PRO
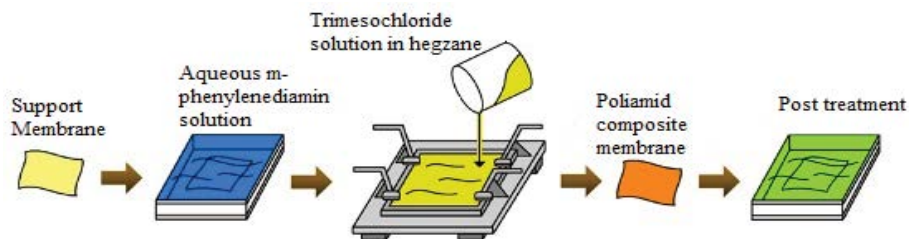
Fig. 3. Thin-film composite coating procedure.
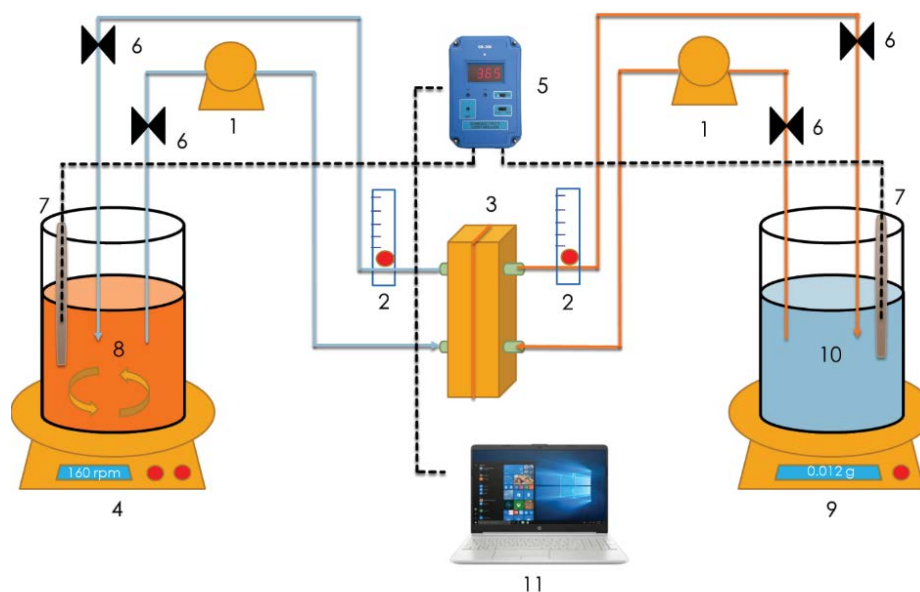
Fig. 4. Schematic of PRO setup (1) circulation pump; (2) flow meter; (3) PRO membrane and module; (4) magnetic stirrer; (5) conductivity meter; (6) inlet/outlet valve; (7) conductivity meter probe; (8) draw solution tank; (9) weighing balance; (10) feed solution tank; (11) computer.
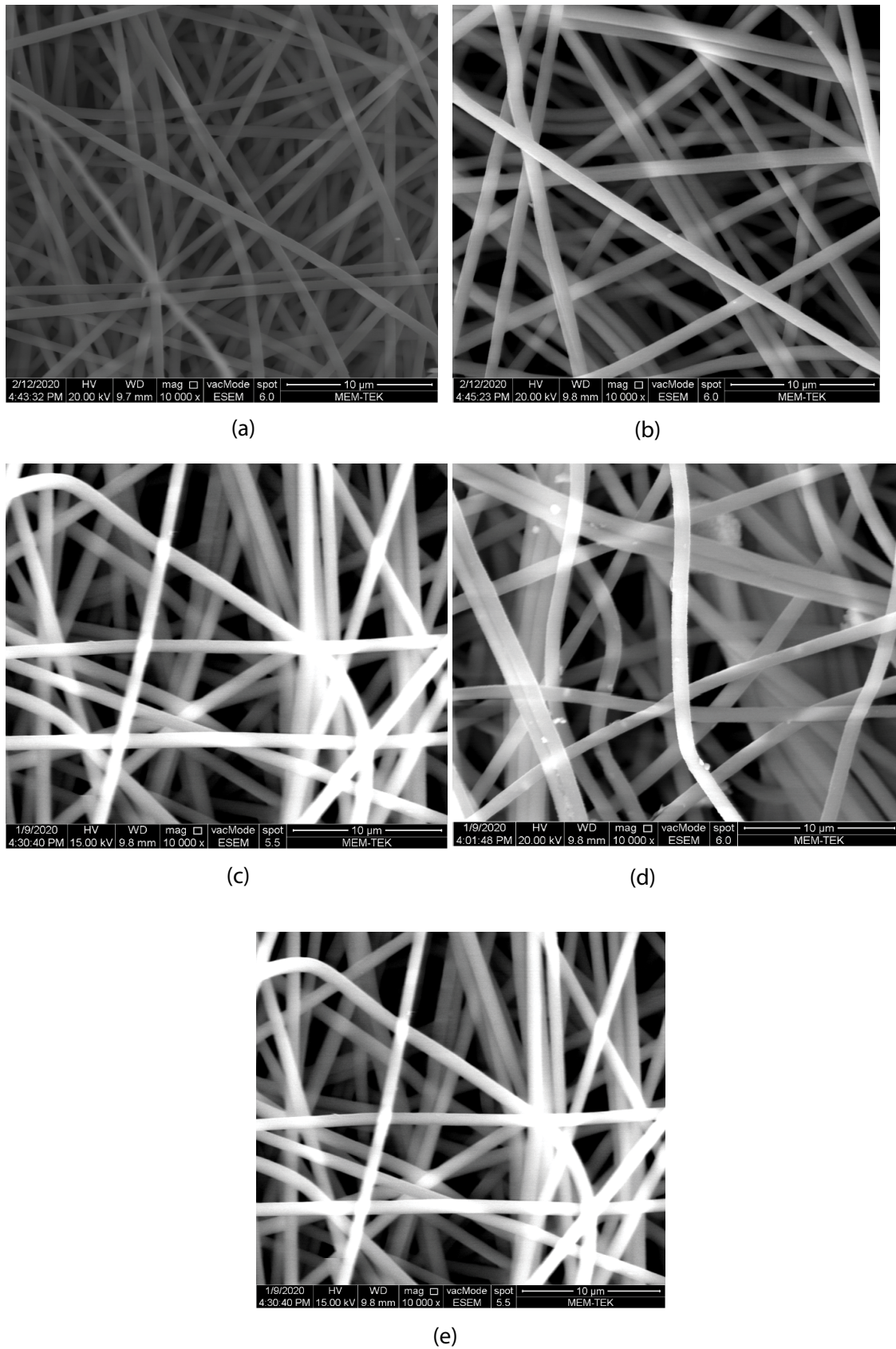
Fig. 5. SEM images of fabricated PAN/CNC nanofiber support membranes. (a) %16 PAN %0 CNC, (b) %16 PAN %1 CNC, (c) %16 PAN %2 CNC, (d) %16 PAN %5 CNC and (e) %16 PAN %10 CNC.
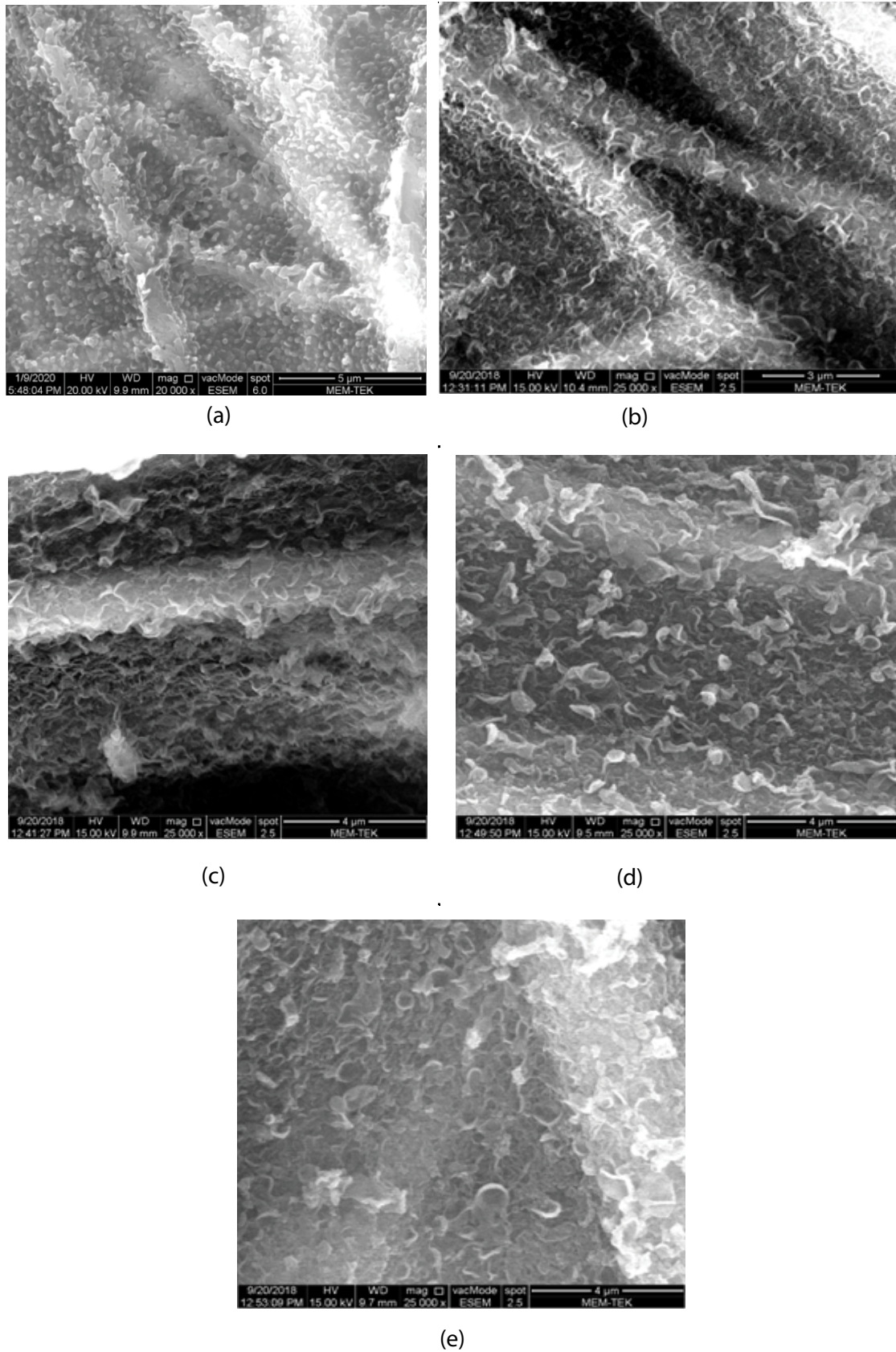
Fig. 6. SEM images of fabricated nanofiber TFC-PRO membranes. (a) 16% PAN 0% CNC, (b) 16% PAN 1% CNC, (c) 16% PAN 2% CNC, (d) 16% PAN 5% CNC and (e) 16% PAN 10% CNC.

process and FO process, a more hydrophilic support layer is desirable as such supports will have less internal concentration polarization and better water flux. More MPD aqueous solution impregnated in pores in supports of the hydrophilic base. In addition, the aqueous MPD solution meniscus was concave in pores after the support containing MPD aqueous solution was dried, and the MPD monomer diffused more slowly out of the pores when contacting TMC solution. The hydrophilic pore wall thus reduced the aggression of the initial MPD "eruption" and resulted in further PA development deeper within support layer pores resulting in improved total route duration for water and solute transport [18].

3.2. Dynamic mechanical analysis of the fabricated membranes

The mechanical properties of CNC/PAN nanocomposite PRO membranes were determined using Seiko DMA Exstar 6100 (Japan). Three specimens of each composition were tested at 25°C, in accordance with the ASTM D638.

Dynamic mechanical analysis of fabricated membranes is performed for different CNC addition ratios. In Fig. 8 results show that an increasing amount of CNC is increased the young's modules of fabricated membranes which is a vital parameter in order to resist high pressure. The reason for this performance increase is the higher viscosity of the polymer solution at higher CNC concentration. The higher the polymer viscosity leads to thicker fiber formation. Thicker fibers make the final membrane structure more rigid to higher pressure and environmental conditions.

3.3. Fourier-transform infrared spectroscopy (FTIR) of the fabricated membranes

In order to verify the chemical structure of organic molecules and the possible structural changes that occur through CNC addition to the PAN phase, Fourier-transform infrared spectroscopy (FTIR) was reported for the dry support layer membrane. FTIR spectrum was measured using
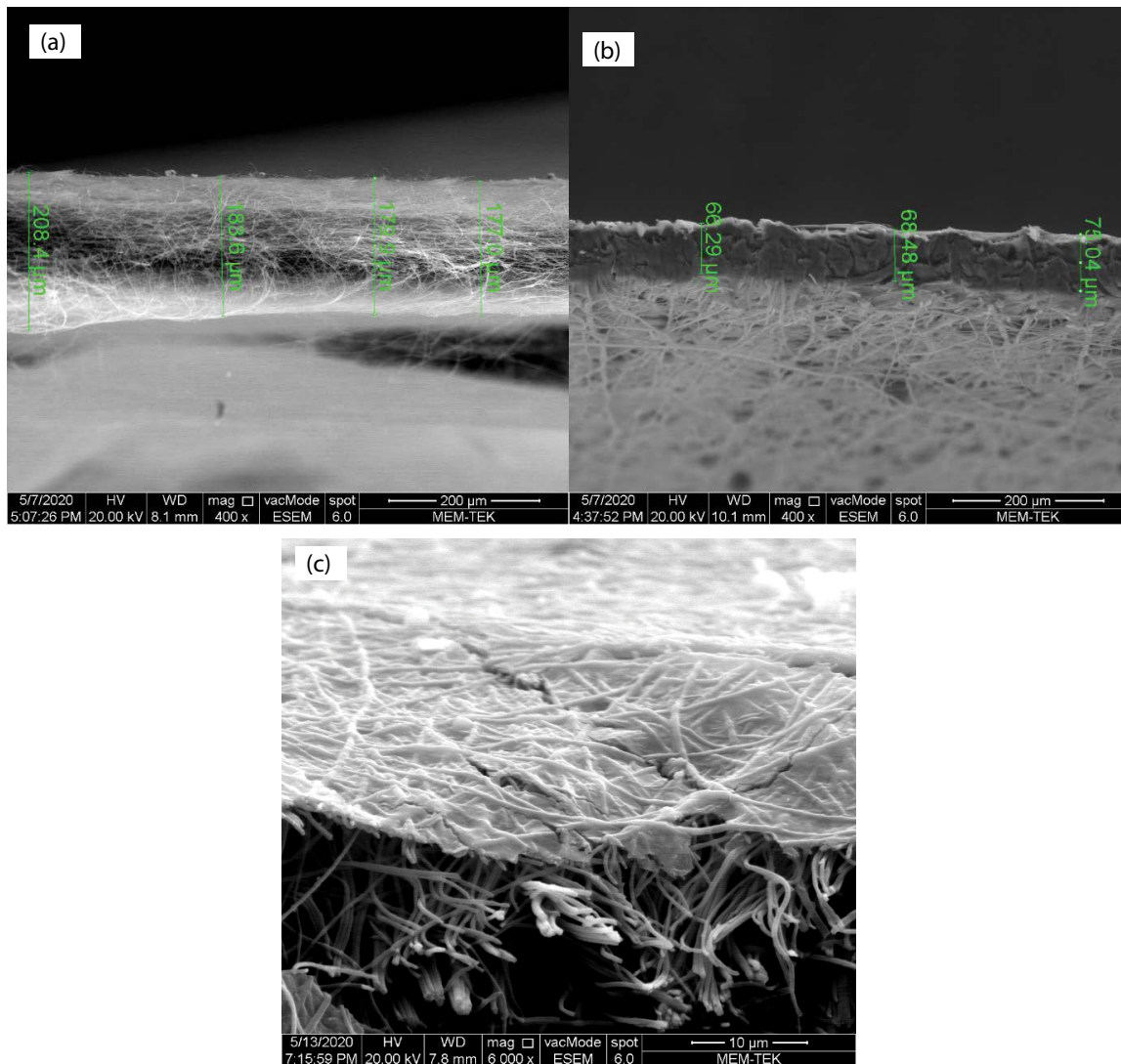
Fig. 7. Cross-section SEM images of fabricated nanofiber TFC-PRO membranes (a), PET non-woven support (b) and cross-view of the polyamide coating (c).

the PerkinElmer Spectrum 100 FTIR Spectrometer, (USA) (650–4,000 cm⁻¹) mode of absorption. Fig. 9 proves that the FTIR spectrum of fabricated membranes proves that with the increasing of crystal nanocellulose addition C–N group gave reaction with the cellulose group and disappear on 1,664.58 cm⁻¹ point.

Due to C=O interconnectivity, which is one feature of lignin and lignin/hemicellulose, the peak of CNC was present at 1,620 cm⁻¹ in the spectrum [19]. Fig. 9 also shows that the PAN spectrum value as 1,452 cm⁻¹ which is the

usual characteristic C–H stretching methylene band and the average vibration of 2,923 cm⁻¹ is the C–H stretching vibration. The vibration average of 2,244 cm⁻¹ belongs to C≡N [20].

3.4. Contact angle analysis of the fabricated membranes

The hydrophilicity of fabricated CNC/PAN nanofiber nanocomposite membranes, 2 µL of DI water drop placed on the membrane surface by contact angle measures using a
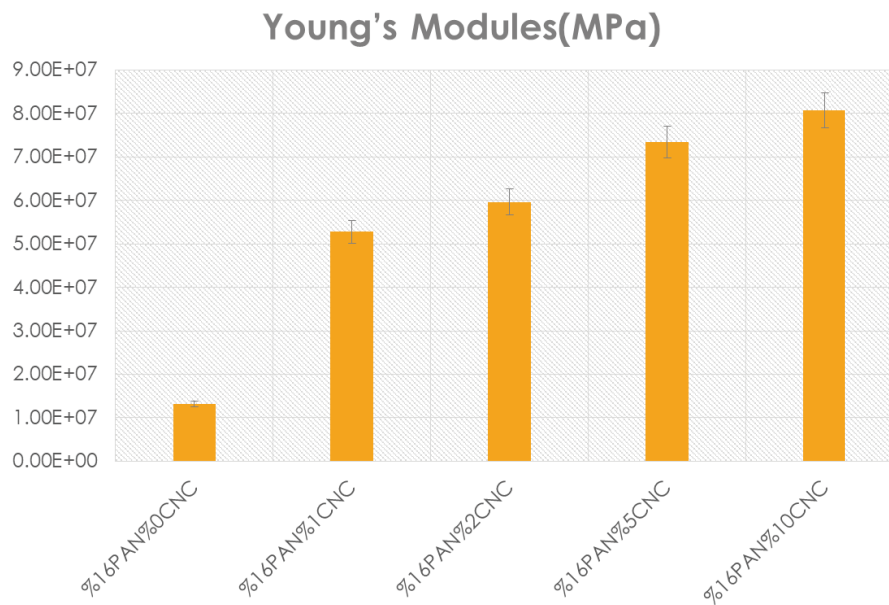
Fig. 8. Young's modules of fabricated membranes.
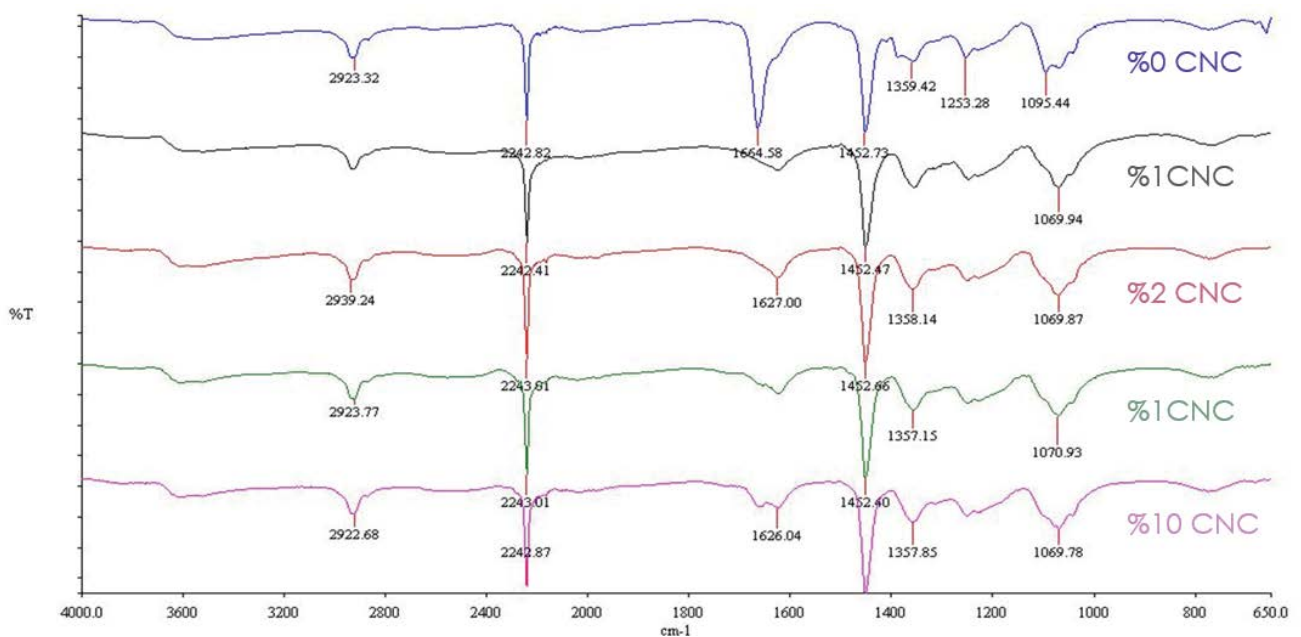
Fig. 9. Comparison of FTIR spectra of fabricated membranes.

goniometer (Attension-KSV-Espoo, Finland). From the three different places on each side of the membrane, 10 images are taken and the mean contact angle is averaged. The scale is 0°–180° and the difference value is ±0.1°. The highest and lowest values were discarded, and the mean value was recorded for the eight remaining angles. According to the results, an increasing amount of CNC to PAN polymer solution, the contact angle of the fabricated membranes show dramatically decrease which helps to increase membrane water flux in the process which is shown in Fig. 10. According to the studies in the literature [21] results show the increasing amount of CNC helps to decrease membrane contact angle value.

3.5. Porometer analysis of the fabricated membranes

Nanofiber membrane porometry is investigated for pore size and distribution. Quantachrome Porofil was used as a weighting agent for porometry measuring with given low surface impedance 16 dyne/cm (Quantachrome Ins., Florida, USA). For porometry measurement, the membranes were classified into 3 cm × 3 cm circles and average results are given in Fig. 11.

Increased polymer molecular weight and viscosity the molecular entanglement of the solution leading to increased fiber diameter [22]. The concentration of the solution is connected to nanofibers diameter and membrane thickness. The diameter and thickness are in effect related to the distribution of the pore size and the pore form. At very low viscosity of the polymer solution, the electrospinning polymer does not have enough entanglements to establish cohesion, which contributes to the forming of droplets. As a result, breakage happens rather than the production of nanofibers. When the concentration of polymer is above the entanglement concentration required for the entanglement of polymer macromolecular chains, beaded nanofibers are formed [23]. An increasing amount of CNC addition into the PAN polymer solution, fabricated nanocomposite nanofiber membranes show a decreasing porosity trend. The reason for smaller pore size after 5% CNC addition, fiber diameter is to increase and pore size distribution decreases.

3.6. Filtration test of the fabricated membranes

A pure water flux test was established in dead-end filtration cells (Sterlitech Corp., Kent, USA). For compaction of the membranes, around 1 L of DI water was filtered under 0.6 bar.

According to the results in the study, an increased amount of CNC in the PAN polymer matrix increased membrane pure water flux. The main reason for pure water increase with increased CNC content in Fig. 12 is hydrophilicity. According to a recent study, more hydrophilic membranes show higher pure water flux [21]. So, it can be concluded that increased CNC content makes PAN/CNC membranes more hydrophilic than pure PAN nanocomposite membranes.

3.7. Reverse osmosis separation performance of fabricated PRO membranes

All TFC-PRO membranes rejected NaCl at more than 94% when tested at 13.8 bar (200 psi) (Fig. 13), making them sufficiently selective for PRO applications and energy generation. The average R was 95.0% ± 1.65% for 0% CNC membranes (n = 2), 94.4% ± 1.50% for 1% CNC membranes (n = 2), 97.0% ± 0.85% for 2% CNC membranes (n = 2), 99.0% ± 1.00% for 5% CNC membranes (n = 2), 98% ± 0.90% for 10% CNC membranes (n = 2). Each bar represents an average obtained from testing of two separately cast membranes.
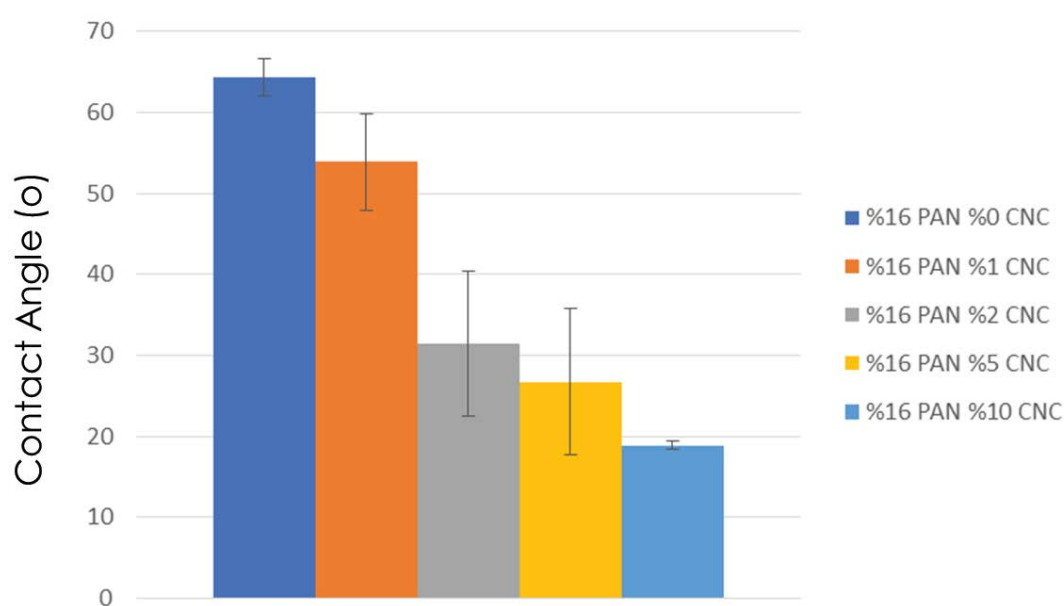
Fig. 10. The contact angle of CNC/PAN nanocomposite nanofiber membranes.
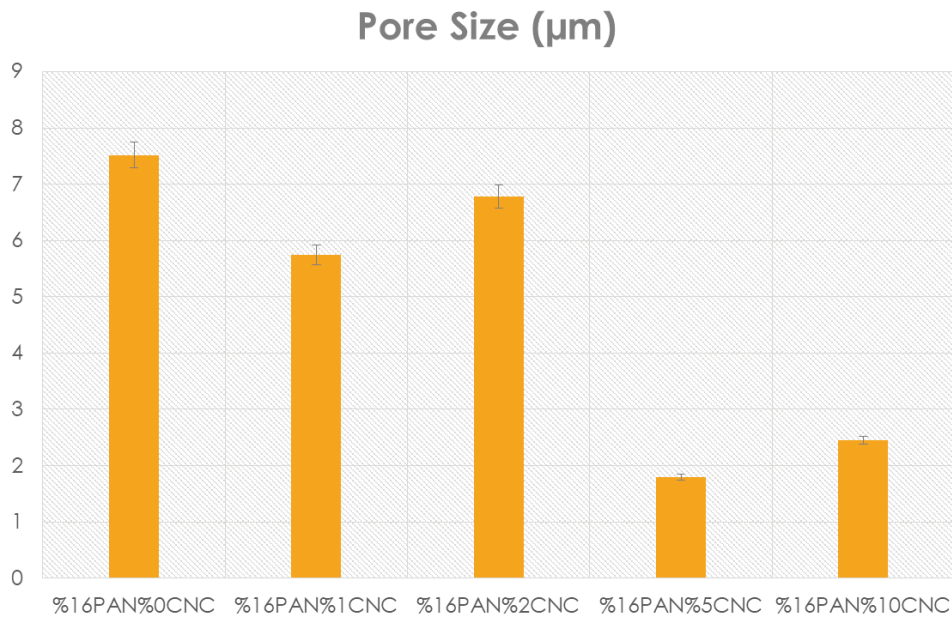
Pore Size (µm)

Fig. 11. Average pore size measurement of CNC/PAN nanocomposite nanofiber membranes.
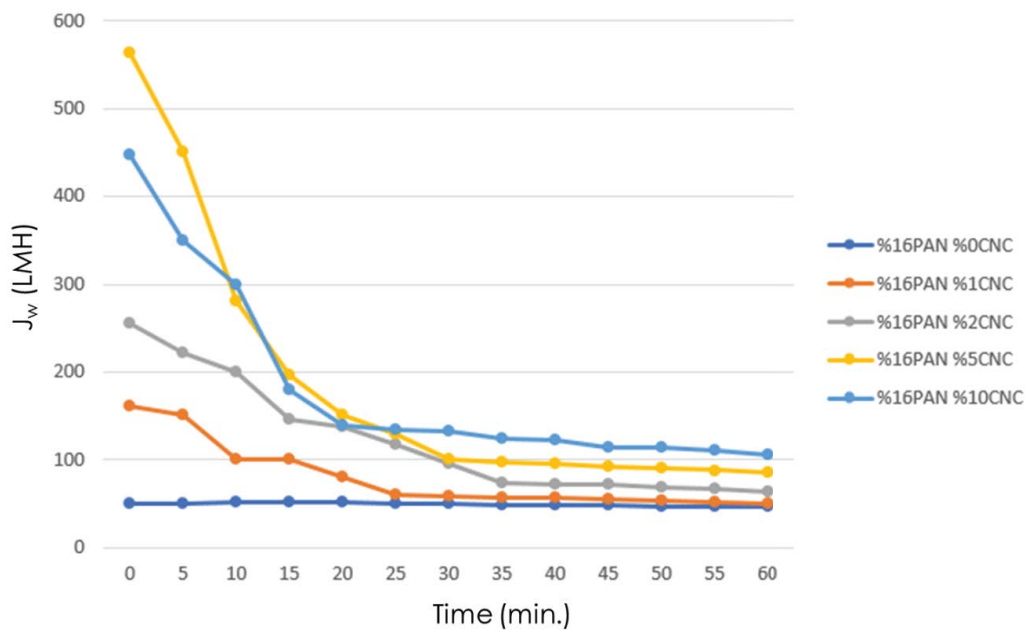
Fig. 12. Comparison of PAN/CNC nanocomposite nanofiber membranes pure water flux.

3.8. PRO test results

The membrane is oriented in the PRO mode when the draw solution is placed against the active layer and the feed solution against the support layer. This mode is typically used in PRO applications where the draw solution is pressurized and therefore requires the porous layer's mechanical support on the membrane's feed side. In traditional PRO systems, salinity in the feed water can generate concentrative results of polarization of internal concentration [24].

Under the same conditions, 5% CNC added PAN nanocomposite nanofiber TFC-PRO membranes perform higher water flux which is shown in Fig. 14. After 60 min of operation, most of the fabricated membranes considerably sustain their original flux.

Reverse salt flux shows salt leakage from the PRO membrane draw solution side to the feed solution side. After quite a while salt leakage dilutes the draw side which leads to a decrease osmotic pressure difference. So, while ideal PRO membrane manufacturing, it is a must to provide the

RO Separation Performance
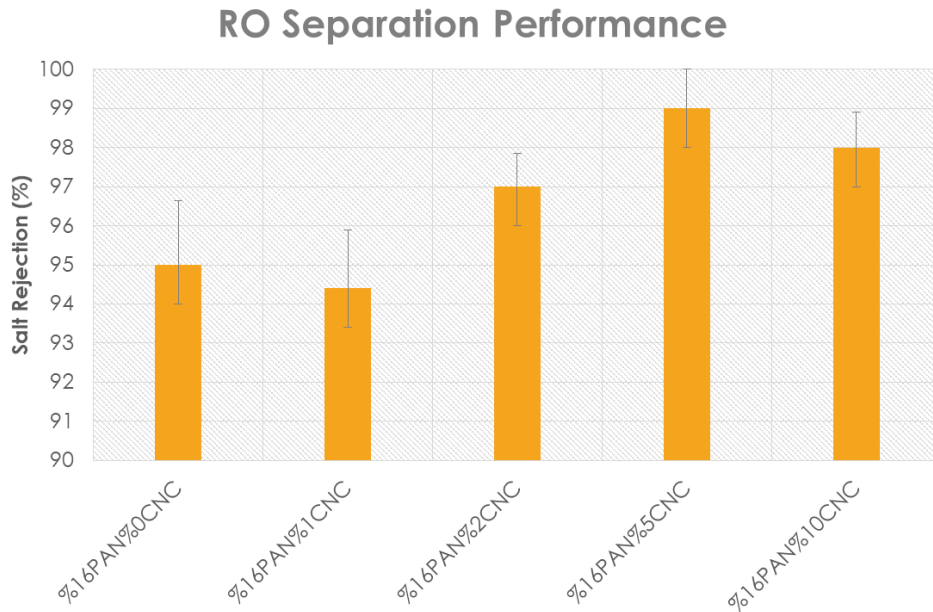
Fig. 13. Comparison of PAN/CNC nanocomposite nanofiber membranes salt rejections.
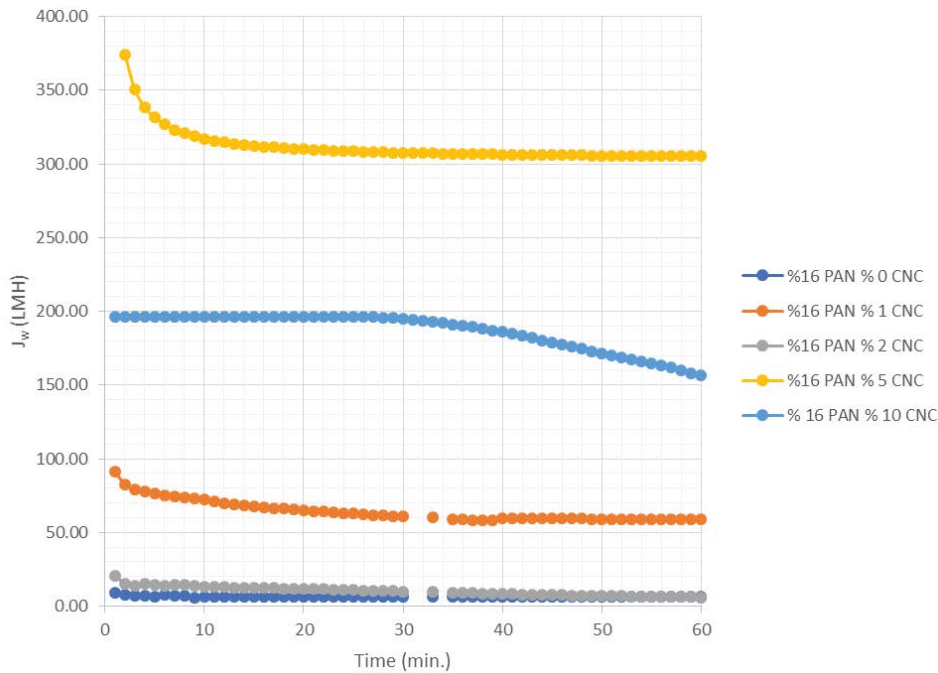
Fig. 14. Fabricated PAN/CNC nanocomposite nanofiber TFC-PRO membranes water flux (J_w).

lowest reverse salt flux and higher water flux. In this study, it can be easily seen in Fig. 15, 5% CNC added PAN nanocomposite nanofiber TFC membranes give the best performance.

Another comparison was made between this study and literature in terms of water flux and reverse salt flux of the membranes for PRO application in Table 2. The results show that fabricated membranes in this study have one of the highest J_w/J_s ratios in the literature.

4. Conclusions

Fabrication of nanofiber PRO was performed successfully electrospinning equipment. Fabricated PRO membranes meet the needs of higher pressures during operation. An increasing the amount of CNC positively affects the young's modules which makes the membrane stronger. FTIR spectra prove that related groups gave reactions with
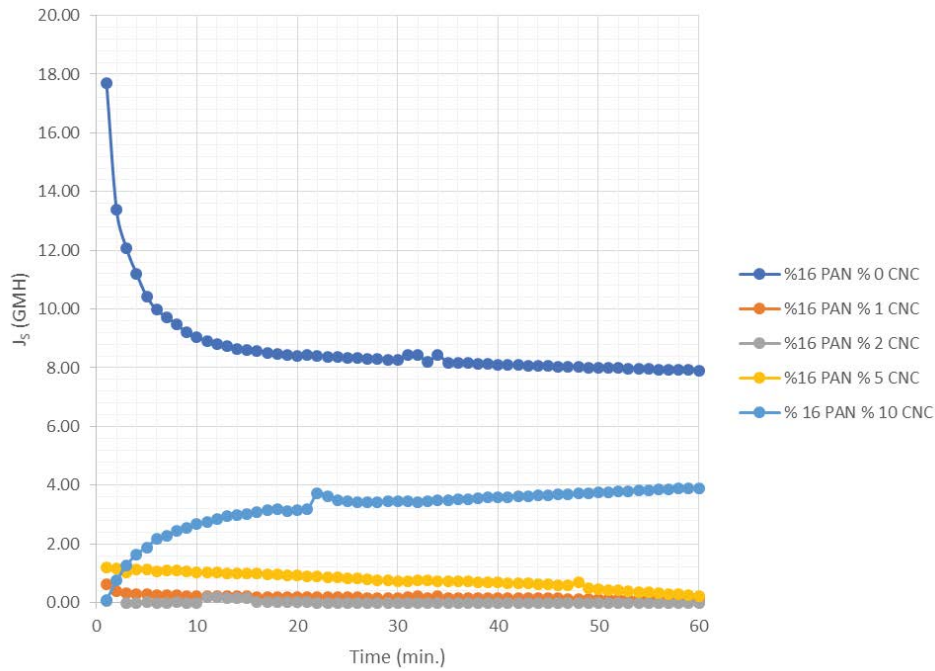
Fig. 15. Fabricated PAN/CNC nanocomposite nanofiber TFC-PRO membranes reverse salt flux (J_s).

Table 2
Comparisons of PRO performance of various TFC membranes with DI water as feed solutions

Membrane	Water flux, J_w (PRO) (LMH)	Reverse salt flux, J_s (PRO) (gMH)	J_s/J_w (g/L)	J_w/J_s (L/g)	Draw solution	References
PAN/CNC nanocomposite TFC membrane (5% CNC)	300	1.5	0.005	200	1.0 M NaCl	This study
FO flat-sheet membrane on sPSU	313	5.3	0.017	58.8	1.0 M NaCl	[25]
Electrospun-PSf-based TFC with PET layer-before adding sodium dodecyl sulfate (SDS)	26	2.26×10^{-3}	0.00008	0.01150	1.5 M NaCl	[26]
Electrospun-PSf-based TFC with PET layer-after adding SDS	33.6	4.62×10^{-2}	0.0013	0.072	1.5 M NaCl	
Electrospun-PSf-based TFC without PET layer-before adding SDS	24.0	8.63	0.359	2.78	1.5 M NaCl	[26]
Electrospun-PSf-based TFC without PET layer-after adding SDS	86.1	36.40	0.422	25.32	1.5 M NaCl	[26]
Asymmetric Cellulose Triacetate Membrane Fabricated by Hydration Technology Innovations LLC	8.10	20.03	2.47	0.4	1.0 M NaCl	CTA-ES HTI data sheet
Thin Film Composite Flat Sheet FO Membrane	19.31	14.78	0.765	1.3	1.0 M NaCl	TFC-ES HTI data sheet
FO flat sheet membrane on cellulose ester substrate	128.8	19.4	0.15	6.67	2.0 M NaCl	[27]
FO flat sheet membrane on sulfonated polyphenylenesulfone (2.5 mole% direct sulfonation) supports	54	8.8	0.163	6.13	2.0 M NaCl	[28]
FO flat sheet membrane on polyethersulfone/sulfonated polysulfone supports	47.5	12.4	0.261	3.83	2.0 M NaCl	[29]

the cellulose groups and change the spectra and it was found out increasing the amount of CNC makes the membrane more hydrophilic. Apart from the FTIR spectrum results, it can be concluded that CNC material is compatible with PAN polymer. Morphology studies performed via SEM equipment were shown that increasing the amount of CNC does not affect dramatically membrane formation until 10% CNC addition. But, in 10% CNC ratio nanofiber formation was broken and formed beads. Regarding the PRO performance tests, 5% CNC addition into the PAN polymer matrix gives superior water flux and obtains the lowest reverse salt flux. Comparison of this study with literature it can be easily seen that PAN/CNC nanocomposite TFC membranes gives maximum water flux and lowest reverse salt flux.

Acknowledgment

References

[1] A. Altaee, A. Sharif, Pressure retarded osmosis: advancement in the process applications for power generation and desalination, Desalination, 356 (2015) 31–46.

[2] G.Z. Ramon, B.J. Feinberg, E.M.V. Hoek, Membrane-based production of salinity-gradient power, Energy Environ. Sci., 4 (2011) 4423.

[3] B.E. Logan, M. Elimelech, Membrane-based processes for sustainable power generation using water, Nature, 4888 (2012) 313–319.

[4] B.B. Sales, F. Liu, O. Schaetzle, C.J.N. Buisman, H.V.M. Hamelers, Electrochemical characterization of a supercapacitor flow cell for power production from salinity gradients, Electrochim. Acta, 86 (2012) 298–304.

[5] J.W. Post, J. Veerman, H.V.M. Hamelers, G.J.W. Euverink, S.J. Metz, K. Nymeijer, C.J.N. Buisman. Salinity-gradient power: evaluation of pressure-retarded osmosis and reverse electrodialysis, J. Membr. Sci., 288 (2007) 218–230.

[6] A. Achilli, A.E. Childress, Pressure retarded osmosis: from the vision of Sidney Loeb to the first prototype installation — review, Desalination, 261 (2010) 205–211.

[7] K.L. Lee, R.W. Baker, H.K. Lonsdale, Membranes for power generation by pressure-retarded osmosis, J. Membr. Sci., 8 (1981) 141–171.

[8] K. Gerstandt, K.-V. Peinemann, S.E. Skilhagen, T. Thorsen, T. Holt, Membrane processes in energy supply for an osmotic power plant, Desalination, 224 (2008) 64–70.

[9] J.M. Deitzel, J. Kleinmeyer, D. Harris, N.C. Beck Tan, The effect of processing variables on the morphology of electrospun nanofibers and textiles, Polymer, 42 (2001) 261–272.

[10] N.M. Julkapli, S. Bagheri, Progress on nanocrystalline cellulose biocomposites, React. Funct. Polym., 112 (2017) 9–21.

[11] M.E. Pasaoglu, I. Koyuncu, Z. Candan, Mechanical Strength Improvement of Polyacrylonitrile (PAN) Nanofiber TFC Pressure Retarded Osmosis (PRO) Membrane Using Cellulose Nanocrystals (CNCs), 9th International Water Association (IWA) Membrane Technology Conference & Exhibition for Water and Wastewater Treatment and Reuse (IWA-MTC 2019), 23–27 June 2019, Toulouse, France, 2019.

[12] W. Helbert, J.Y. Cavaillé, A. Dufresne, Thermoplastic nanocomposites filled with wheat straw cellulose whiskers. Part I: processing and mechanical behavior, Polym. Compos., 17 (1996) 604–611.

[13] K. Abe, S. Iwamoto, H. Yano, Obtaining cellulose nanofibers with a uniform width of 15 nm from wood, Biomacromolecules, 8 (2007) 3276–3278.

[14] M. Börjesson, G. Westman, Crystalline Nanocellulose — Preparation, Modification, and Properties, M. Poletto, H.L. Ornaghi Jr., Eds., Cellulose-Fundamental Aspects and Current Trends, IntechOpen, London, 2015, pp. 161–191.

[15] Y. Wyart, G. Georges, C. Deumié, C. Amra, P. Moulin, Membrane characterization by microscopic methods: multiscale structure, J. Membr. Sci., 315 (2008) 82–92.

[16] Z.-K. Xu, X.-J. Huang, L.-S. Wan, Techniques for Membrane Surface Characterization, In: Surface Engineering of Polymer Membranes (Advanced Topics in Science and Technology in China), Springer, Berlin, Heidelberg, 2009, p. 333.

[17] W.J. Lau, A.F. Ismail, P.S. Goh, N. Hilal, B.S. Ooi, Characterization methods of thin film composite nano-filtration membranes, Sep. Purif. Rev., 44 (2015) 135–156.

[18] F. Liu, L.L. Wang, D.W. Li, Q.S. Liu, B.Y. Deng, A review: the effect of the microporous support during interfacial polymerization on the morphology and performance of a thin film composite membrane for liquid purification, RSC Adv., 9 (2019) 35417–35428.

[19] M. Asrofi, H. Abral, A. Kasim, A. Pratoto, XRD and FTIR studies of nanocrystalline cellulose from Water Hyacinth (*Eichornia crassipes*) fiber, J. Metastable Nanocryst. Mater., 29 (2017) 9–16.

[20] S.X. Jin, J.L. Yu, Y.S. Zheng, W.-Y. Wang, B.J. Xin, C.-W. Kan. Preparation and characterization of electrospun PAN/PSA carbonized nanofibers: experiment and simulation study, Nanomaterials (Basel, Switzerland), 8 (2018) 821.

[21] L.M. Bai, N. Bossa, F.S. Qu, J. Winglee, G.B. Li, K. Sun, H. Liang, M.R. Wiesner, Comparison of hydrophilicity and mechanical properties of nanocomposite membranes with cellulose nanocrystals and carbon nanotubes, Environ. Sci. Technol., 51 (2017) 253–262.

[22] M. Yousefzadeh, Modeling and Simulation of the Electrospinning Process, M. Afshari, Ed., Electrospun Nanofibers, A Volume in Woodhead Publishing Series in Textiles, Duxford, Cambridge, Kidlington, 2017, pp. 277–301.

[23] S.S. Murthe, M.S.M. Saheed, V. Perumal, M.S.M. Saheed, N.M. Mohamed, Electrospun Nanofibers for Biosensing Applications, S.C.B. Gopinath, T. Lakshmipriya, Ed., Nanobiosensors for Biomolecular Targeting: A Volume in Micro and Nano Technologies, Elsevier, Amsterdam, Oxford, Massachusetts, 2019, pp. 253–267.

[24] J.R. McCutcheon, M. Elimelech, Influence of membrane support layer hydrophobicity on water flux in osmotically driven membrane processes, J. Membr. Sci., 318 (2008) 458–466.

[25] R.M. El Khaldi, M.E. Pasaoglu, S. Guclu, Y.Z. Menceloglu, R. Ozdogan, M. Celebi, M.A. Kaya, I. Koyuncu, Fabrication of high-performance nanofiber-based FO membranes, Desal. Water Treat., 147 (2019) 56–72.

[26] N.N. Bui, M.L. Lind, E.M.V. Hoek, J.R. McCutheon, Electrospun nanofiber supported thin film composite membranes for engineered osmosis, J. Membr. Sci., 385–386 (2011) 10–19.

[27] R.C. Ong, T.-S. Chung, J.S. de Wit, B.J. Helmer, Novel cellulose ester substrates for high performance flat-sheet thin-film composite (TFC) forward osmosis (FO) membranes, J. Membr. Sci., 473 (2015) 63–71.

[28] N. Widjojo, T.-S. Chung, M. Weber, C. Maletzko, V. Warzelhan, A sulfonated poly-phenylenesulfone (sPPSU) as the supporting substrate in thin film composite (TFC) membranes with enhanced performance for forward osmosis (FO), Chem. Eng., 220 (2013) 15–23.

[29] K.Y. Wang, T.-S. Chung, G. Amy, Developing thin-film-composite forward osmosis membranes on the PES/SPSf substrate through interfacial polymerization, AIChE J., 58 (2012) 770–781.